BMC Pulmonary Medicine

RESEARCH

Open Access

Longitudinal change of idiopathic inflammatory myopathy-associated interstitial lung disease on high-resolution computed tomography, a prospective cohort study

Yuhui Qiang[1,2†], Hongyi Wang[2,3†], Yifei Ni[3,4], Jianping Wang[1,4], Anqi Liu[3,4], Jie Du[3,4], Linfeng Xi[1,2], Yinan Hu[1,2], Yanhong Ren[1,2], Bingbing Xie[1,2], Shiyao Wang[1,2], Jing Geng[1,2], Min Liu[4*] and Huaping Dai[1,2,3*]

Abstract

Background This study aimed to investigate longitudinal change of idiopathic inflammatory myopathy-associated interstitial lung disease (IIM-ILD) on high-resolution computed tomography (HRCT).

Methods This prospective cohort study was undertaken involving 514 IIM-ILD patients (367 females; median age 54 years) from 2016 to 2022. Deep learning algorithms were employed to quantify interstitial lesions on HRCT, while clinical parameters including pulmonary function tests, serum biomarkers, and arterial blood gas analysis were also considered.

Results The study identified anti-MDA5 antibody positivity (OR: 10.46, 95% CI: 3.40–32.22), reduced FVC (OR: 0.91, 95% CI: 0.84–0.98), and extensive ground-glass opacity (GGO) (OR: 1.07, 95% CI: 1.01–1.13)/ reticulation (OR: 1.23, 95% CI: 1.07–1.41) involvement as independent risk factors for rapidly progressive interstitial lung disease (RP-ILD) within IIM. During the rapid progressive period of RP-ILD, anti-MDA5-positive dermatomyositis (MDA5 + DM) showed greater progression in fibrotic, inflammatory, and emphysema lesions compared to anti-synthetase syndrome (ASS). In the slow progressive period, MDA5 + DM tended towards chronic fibrosis, while ASS exhibited overall improvement. The extent of lesion increase in non-RP-ILD patients is significantly smaller than in those who have experienced RP. Reticular and consolidation changes were strongly correlated with variations in VC%, FVC%, and FEV_1%, and moderately associated with changes in TLC and DL_{CO}. The prognostic impact of GGO proportion on adverse outcomes intensified with longer follow-up durations, with each 1-unit increase in whole-lung GGO proportion linked to a 0.56% higher risk of adverse outcomes (HR: 1.0056, 95% CI: 1.001–1.010).

†Yuhui Qiang and Hongyi Wang contributed equally.

*Correspondence:
Min Liu
mikie0763@126.com
Huaping Dai
daihuaping@ccmu.edu.cn

Full list of author information is available at the end of the article

Conclusions IIM-ILD cases with prior rapid progression will develop chronic fibrotic trajectories with persistent inflammation compared to non-progressive cases. ASS is characterized by sustained inflammatory activity in imaging manifestations, whereas MDA5 + DM shows post-acute fibrotic remodeling following initial injury. Longitudinal GGO emerges as a critical prognostic indicator, demonstrating time-dependent cumulative risk effects.

Keywords Idiopathic inflammatory myopathy, Rapidly progressive interstitial lung disease, High-resolution computed tomography, Quantitative CT, Longitudinal analysis

Background

Idiopathic inflammatory myopathy-associated interstitial lung disease (IIM-ILD) represents a heterogeneous group of autoimmune disorders characterized by predominant pulmonary manifestations, with marked variability in clinical progression and prognosis. Within this disease spectrum, anti-synthetase syndrome (ASS) and anti-melanoma differentiation-associated gene 5 antibody-positive dermatomyositis (MDA5 + DM) emerge as distinct clinical entities with divergent prognostic implications [1–5]. Rapidly progressive interstitial lung disease (RP-ILD), a critical phenotype of IIM-ILD, is distinguished by acute deterioration and high mortality, emerging as a major contributor to poor outcomes [6–10]. Despite significant progress in establishing multidisciplinary discussion (MDD)-based diagnostic criteria for IIM-ILD, critical knowledge gaps persist regarding key imaging features and pathophysiological mechanisms. Particularly, the transition dynamics between inflammatory and fibrotic phases remain poorly characterized, and substantial heterogeneity across disease subtypes continues to challenge both mechanistic understanding and clinical management.

High-resolution computed tomography (HRCT), a key method for ILD diagnosis and evaluation, plays a pivotal role in characterizing spatial distributions and morphological patterns of lung lesions. Recent advances in artificial intelligence (AI), especially deep learning techniques [11–14] for automated lesion segmentation and volumetric quantification in HRCT, have opened new avenues for understanding the link between imaging features and clinical manifestations in IIM-ILD. However, existing studies predominantly focus on cross-sectional analyses of baseline imaging features, leaving significant gaps in understanding the longitudinal evolution of quantitative CT (QCT) parameters during disease progression, their correlations with pulmonary function, and the identification of time-dependent prognostic biomarkers [15–18]. Furthermore, the potential divergence in imaging patterns and disease trajectories between ASS and MDA5 + DM, likely driven by antibody-mediated immune pathway differences, has yet to be systematically investigated.

Against this backdrop, this study constructs a prospective longitudinal cohort to achieve three objectives: (1) to develop a predictive model for RP-ILD using multimodal data (serological, pulmonary function, QCT) to identify critical risk factors; (2) to elucidate distinct imaging evolution patterns and mechanistic divergences between ASS and MDA5 + DM across disease progression phases; (3) to evaluate the prognostic value of HRCT-derived biomarkers to inform personalized therapeutic strategies and dynamic monitoring protocols.

Methods

Study cohort and design

This single-center prospective cohort study was approved by the Ethics Committee of our Hospital (No. 2017-25), and informed consent was obtained from all participants. Consecutive patients diagnosed with IIM-ILD between January 1, 2016, and January 31, 2022, were enrolled. The diagnosis of IIM-ILD was confirmed through MDD in accordance with established criteria for interstitial pneumonias [9, 19, 20]. DM was diagnosed based on the Bohan and Peter criteria and the 239th European Neuromuscular Centre International Workshop guidelines [21, 22]. ASS was defined by the presence of anti-aminoacyl-tRNA synthetase (ARS) antibodies and at least one clinical triad feature (myositis, arthritis, or ILD) [23]. Anti-ARS and anti-MDA5 antibodies were detected using a commercial line immunoassay (EUROLINE Myositis Profile, Order No. DL 1530-4 G#, EUROIMMUN, Lübeck, Germany) according to the manufacturer's instructions. The assay comprehensively tested for IgG antibodies against the following antigens: Mi-2α, Mi-2β, TIF1γ, MDA5, NXP2, SAE1, Ku, PM-Scl100, PM-Scl75, Jo-1, SRP, PL-7, PL-12, EJ, OJ, and Ro-52. Inclusion criteria: (1) age ≥ 18 years; (2) confirmed diagnosis of ASS or MDA5 + DM; (3) baseline HRCT performed at our hospital prior to treatment. Exclusion criteria: (1) HRCT artifacts impairing lesion assessment; (2) insufficient clinical data to determine RP-ILD status; (3) loss to follow-up. Figure 1 is the flow chart of this study.

Definition of subgroups

RP-ILD was defined per modified ATS criteria for idiopathic pulmonary fibrosis [24], requiring ≥ 2 of the following within 3 months of symptom onset: (I) worsening dyspnea; (II) physiological decline (≥ 10% reduction in vital capacity [VC] or ≥ 1.33 kPa decrease in PaO_2); (III) the progression of ground-glass opacity (GGO), consolidation, reticular pattern, or honeycombing shown on HRCT. Meanwhile, non-RP-ILD exhibits a gradual

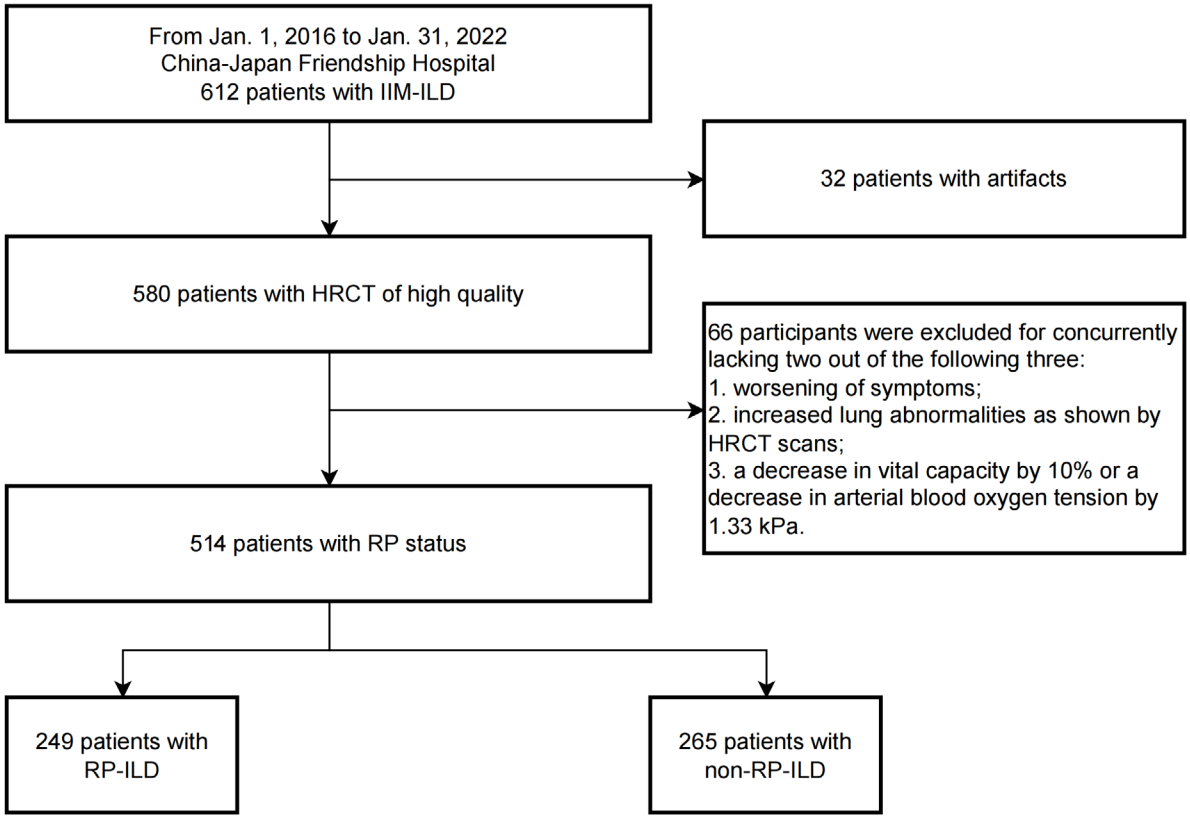

Fig. 1 Flow diagram of eligibility criteria. *IIM-ILD* Idiopathic inflammatory myopathy related interstitial lung disease, *HRCT* High-resolution computed tomography, *RP-ILD* Rapidly progressive interstitial lung disease, *non-RP-ILD* Non rapidly progressive interstitial lung disease

decline in the disease after 3 months or remains relatively stable for an extended period. Disease stages were categorized as: rapid progressive period (baseline to 3 months post-diagnosis for RP-ILD), slow progressive period (stable/slowly progressive disease beyond 3 months post-RP-ILD diagnosis), and non-progressive period (for non-RP-ILD patients who never met the criteria for rapid progression).

Pulmonary function test

Pulmonary function test (PFT) (MasterScreen; Vyaire Medical GmbH, Germany) was performed within 1 week of HRCT. Measurements included predicted vital capacity (VC%), forced vital capacity (FVC%), forced expiratory volume in 1 s (FEV_1%), FEV_1/FVC ratio, total lung capacity (TLC%), and diffusing capacity for carbon monoxide (DL_{CO}%), adhering to ERS/ATS standards [25, 26]. Arterial blood gas analysis (arterial oxygen pressure [PaO_2], arterial carbon dioxide pressure [$PaCO_2$]) was conducted using standardized protocols [27].

HRCT

HRCT scans were acquired using multi-detector CT systems (LightSpeed VCT/64, GE Healthcare; Toshiba Aquilion ONE TSX-301 C/320; Philips iCT/256; Siemens FLASH Dual Source CT) in supine position during breath-hold. Parameters included: 100–120 kV tube voltage, 100–300 mAs tube current, 0.625–1 mm slice thickness, 39.37 mm/s table speed, and 0.8-second gantry rotation. Images were reconstructed at 1 mm slice thickness.

Quantitative CT analysis

HRCT images in the Digital Imaging and Communications in Medicine format were transferred to an in-house AI workstation (CT quantitative system: SIMBIO-T, Hangzhou Smart Intelligent Technology Co., Ltd., Hanzhou, China) for automatic quantitative analysis of lung parenchyma, texture, and radiomics parameters, as shown in Fig. 2 (uncolored HRCT images with annotated regions identified by the software are provided in Figure S1). To ensure segmentation accuracy, a rigorous quality control protocol was implemented: all automated segmentation results were independently reviewed visually

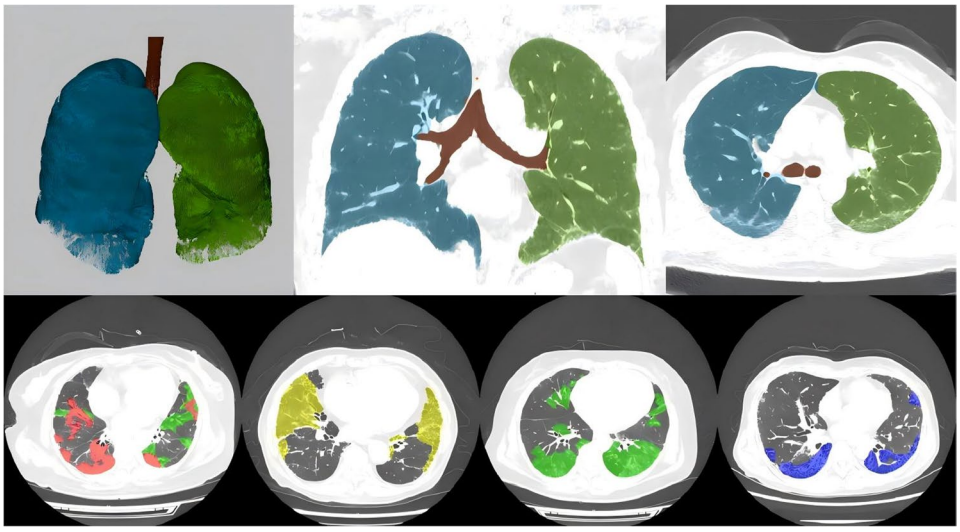

Fig. 2 Segmentation diagram of pulmonary structures. Top panel: Automated lung segmentation using a 3D U-Net based model, accompanied by three-dimensional schematic visualization of pulmonary lobar anatomy. Bottom panel: Segmentation of interstitial lung disease imaging features: Red-Consolidation; Green-Ground-glass opacity; Yellow-Honeycombing; Blue-Reticular pattern

by two board-certified thoracic radiologists with 9 and 15 years of experience, respectively. In cases of inaccurate automatic segmentation, manual corrections were applied following consensus. To evaluate inter-reader agreement, both radiologists independently assessed a randomly selected subset of 30 cases, demonstrating excellent consistency in their approval of segmentation results (Intraclass Correlation Coefficient = 0.87). Additionally, intra-reader consistency was evaluated by having one radiologist re-analyze the same subset after a 4-week interval, showing high reproducibility (ICC = 0.92). Lesion volume was quantified across three vertical lung divisions and expressed as a percentage of total lung volume.

Statistical analysis

Baseline characteristics were summarized using descriptive statistics. Continuous variables (mean ± SD or median [IQR]) were compared via t-tests or Mann-Whitney U tests based on normality (Kolmogorov-Smirnov test). Categorical variables (counts [%]) were analyzed using chi-square or Fisher's exact tests. Multivariable logistic regression was used to identify independent risk factors for RP-ILD. Results are reported as odds ratios (OR) with 95% confidence intervals (CI). For survival analysis, Cox proportional hazards models with time-dependent interactions were used to assess associations between imaging features and prognosis, reported as hazard ratios (HR) and 95% CI. Candidate variables were selected based on univariate significance ($P < 0.1$) or established clinical importance from the literature, and the final model was constructed via bidirectional stepwise selection ($P < 0.05$ for retention). Multicollinearity among the input variables was assessed using the Variance Inflation Factor (VIF), and all variables included in the multivariate models exhibited VIF values below 10. Linear mixed-effects models assessed lesion progression across disease stages, incorporating random individual effects and fixed time effects. Spearman's rank correlation evaluated associations between QCT features and pulmonary function changes. Model discrimination was evaluated via Harrell's C-index. All analyses were performed using R (version 4.4.1, R Foundation for Statistical Computing, Vienna, Austria). A two-tailed $P < 0.05$ was considered statistically significant.

Results

Study population

612 patients with IIM-ILD between January 1, 2016, and January 1, 2022 were initially enrolled at our hospital. After excluding 32 patients with HRCT artifacts and 66 patients with insufficient clinical data to determine RP-ILD status, 514 IIM-ILD patients (367 females; median age 54 years) were included in the final analysis. Among them, 249 patients (165 females; median age 55 years) suffered from RP-ILD. Baseline demographic, pulmonary function, arterial blood gas, interstitial lesions, and inflammatory marker data are summarized in Table 1. To address missing data, we performed multiple imputation using chained equations (MICE) in covariates. The imputation model included all variables used in the primary analysis to preserve the uncertainty around the missing values [28]. Compared to non-RP-ILD patients, RP-ILD patients exhibited a higher prevalence of anti-MDA5 antibody positivity ($P < 0.001$), worse pulmonary volume, ventilation, and diffusion capacity (all $P < 0.001$), lower

Table 1 Characteristics of included patients with idiopathic inflammation myopathy*

Characteristics	Missing value number	Missing value proportion	non-RP-ILD group	RP-ILD group	*P*-value
n			265	249	
Female, n (%)	0	0%	202 (39.53%)	165 (32.28%)	**0.015**
Age, median (IQR)	0	0%	54.00 (46.00, 60.00)	55.00 (47.50, 63.00)	**0.043**
Subtype, n (%)	0	0%			**< 0.001**
ASS			211 (41.05%)	146 (28.40%)	
MDA5 + DM			54 (10.51%)	103 (20.04%)	
Smoke, n (%)	0	0%			**0.005**
Current			3 (2.63)	6 (9.52)	
Former			3 (2.63)	7 (11.11)	
Never			108 (94.74)	50 (79.37)	
Pulmonary function tests					
VC%, median (IQR)	180	35.0%	76.65 (64.775, 89.45)	68.40 (57.10, 79.00)	**< 0.001**
FVC%, median (IQR)	168	32.7%	77.95 (65.40, 91.08)	69.65 (56.33, 81.55)	**< 0.001**
FEV_1%, median (IQR)	167	32.5%	76.10 (63.10, 86.88)	67.45 (55.93, 79.75)	**< 0.001**
FEV_1/FVC%, median (IQR)			80.55 (76.37, 84.86)	81.28 (77.02, 86.15)	0.53
TLC%, median (IQR)	184	35.8%	73.3 (62.95, 83.25)	65.35 (54.83, 77.65)	**< 0.001**
DL_{CO}%, median (IQR)	174	33.9%	61.70 (51.05, 71.65)	50.55 (43.15, 60.28)	**< 0.001**
PaO_2, median (IQR)	91	17.7%	87.60 (80.00, 95.00)	80.25 (71.43, 91.65)	**< 0.001**
$PaCO_2$, median (IQR)	93	18.1%	37.90 (35.20, 40.80)	36.45 (33.70, 39.78)	**0.002**
QCT markers					
Emphysema%, median (IQR)	0	0%	0.05 (0.02, 0.19)	0.09 (0.03, 0.31)	**< 0.001**
Consolidation%, median (IQR)	0	0%	0.13 (0.04, 0.39)	0.27 (0.10, 0.59)	**< 0.001**
Ground glass opacity%, median (IQR)	0	0%	2.46 (0.79, 7.29)	5.42 (1.41, 14.68)	**< 0.001**
Reticular%, median (IQR)	0	0%	3.03 (1.22, 5.90)	5.01 (2.25, 9.38)	**< 0.001**
Honeycomb%, median (IQR)	0	0%	0.02 (0.00, 0.07)	0.05 (0.01, 0.19)	**< 0.001**
Serum biomarkers					
CK (IU/L), median (IQR)	158	30.7%	62.00 (33.00, 174.50)	50.00 (27.00, 136.00)	**0.045**
CRP (mg/L), median (IQR)	199	38.7%	0.38 (0.21, 0.98)	0.46 (0.26, 1.01)	0.228
ESR (mm/h), median (IQR)	165	32.1%	16.00 (8.50, 28.00)	17.50 (9.00, 30.00)	0.321
FET (ng/mL), median (IQR)	247	48.1%	151.85 (60.43, 369.35)	359.10 (109.85, 943.45)	**< 0.001**
LDH (IU/L), median (IQR)	159	30.9%	252.00 (197.00, 321.50)	282.00 (229.00, 355.50)	**< 0.001**
ALT (IU/L), median (IQR)	94	18.3%	27.50 (17.25, 47.75)	34.00 (22.00, 59.00)	**0.002**
AST (IU/L), median (IQR)	94	18.3%	23.50 (17.00, 37.00)	26.00 (18.00, 45.00)	0.061

*Bold values indicate statistical significance at $P < 0.05$. *non-RP-ILD* Non rapidly progressive interstitial lung disease, *RP-ILD* Rapidly progressive interstitial lung disease, *ASS* Anti-synthetase syndrome, *MDA5 + DM* Anti-melanoma differentiation-associated gene 5 antibody-positive dermatomyositis, *VC%* The proportion of actual value to the expected value for vital capacity, *FVC%* The proportion of actual value to the expected value for forced vital capacity, FEV_1% The proportion of actual value to the expected value for forced expiratory volume in the first second, FEV_1/*FVC* The proportion of forced expiratory volume in the first second to the forced vital capacity, *TLC%* The proportion of actual value to the expected value for total lung capacity, DL_{CO}% The proportion of actual value to the expected value for carbon monoxide diffusing capacity, PaO_2 Arterial oxygen pressure, $PaCO_2$ Arterial carbon dioxide pressure, *CK* Creatine kinase, *CRP* C-reactive protein, *ESR* Erythrocyte sedimentation rate, *FET* Ferritin, *LDH* Lactic dehydrogenase, *ALT* Alanine aminotransferase, *AST* Aspartate aminotransferase

PaO_2 ($P < 0.001$), greater extent of emphysema and interstitial lesions (all $P < 0.001$), and elevated levels of creatine kinase ($P = 0.045$), serum ferritin ($P < 0.001$), lactate dehydrogenase ($P < 0.001$), and alanine aminotransferase ($P = 0.002$) at baseline.

Subgroup analyses

Demographic, pulmonary function, interstitial lesions, and inflammatory marker profiles for ASS and MDA5 + DM subgroups are detailed in Tables S1 and S2. Among ASS group, RP-ILD patients were older ($P = 0.013$), had higher C-reactive protein levels ($P = 0.046$), worse pulmonary ventilation/diffusion capacity (all $P < 0.001$), and more emphysema ($P = 0.002$) and interstitial lesion (all $P < 0.001$) compared to non-RP-ILD patients. In MDA5 + DM group, RP-ILD patients were older ($P = 0.011$) and had higher serum ferritin ($P < 0.001$), lactate dehydrogenase ($P = 0.005$), and alanine aminotransferase levels ($P = 0.034$), lower FVC% ($P = 0.049$) and VC% ($P = 0.029$), and more extensive interstitial lesions (*P*: <0.001–0.017).

Risk factors for RP-ILD

Multivariable logistic regression (Table 2) identified anti-MDA5 antibody positivity (OR: 10.46, 95% CI: 3.40–32.22), reduced VC% (OR: 0.91, 95% CI: 0.84–0.98), and

Table 2 Risk factors for rapidly progressing interstitial lung disease*

	OR (95% CI)	*P*-value
MDA5	10.46 (3.40 ~ 32.22)	**< 0.001**
VC%	0.91 (0.84 ~ 0.98)	**0.013**
FEV_1%	1.06 (0.99 ~ 1.14)	0.085
Ground glass opacity%	1.07 (1.01 ~ 1.13)	**0.039**
Reticular%	1.23 (1.07 ~ 1.41)	**0.004**
LDH (IU/L)	1.00 (0.99 ~ 1.00)	0.136
AST (IU/L)	1.01 (1.00 ~ 1.03)	0.154

*Bold values indicate statistical significance at $P < 0.05$. *OR* Odds ratio, *CI* Confidence interval, *MDA5* Anti-melanoma differentiation associated protein 5, *VC%* The proportion of actual value to the expected value for vital capacity, *FEV_1%* The proportion of actual value to the expected value for forced expiratory volume in the first second, *LDH* Lactic dehydrogenase, *AST* Aspartate aminotransferase

greater involvement of GGO (OR: 1.07, 95% CI: 1.01–1.13) and reticular pattern (OR: 1.23, 95% CI: 1.07–1.41) as independent risk factors for RP-ILD.

Longitudinal HRCT changes across disease stages

We detailed the cohort's survival outcomes and HRCT follow-up rates to address the longitudinal nature of this study. The number of deceased cases at predetermined intervals for each disease subtype is presented in Table S3. Concurrently, the cumulative deaths and actual sample size of patients who successfully received HRCT examinations at each follow-up time point are provided in Table 3. Specifically, in the MDA5 + DM-RP-ILD subgroup, there were 20 deaths, with 9 occurring during the rapid progressive period and 11 during the slow progressive period; the actual sample sizes for HRCT examination at follow-up were 103 during the rapid progressive period and 94 during the slow progressive period. In the ASS-RP-ILD subgroup, there were 20 deaths, with 2 during the rapid progressive period and 18 during the slow progressive period; the actual sample sizes were 146 during the rapid progressive period and 144 during the slow progressive period. For the MDA5 + DM-non-RP-ILD subgroup, there was 1 death with an actual HRCT sample size of 54. In the ASS-non-RP-ILD subgroup, there were 16 deaths with an actual HRCT sample size of 211. These tables offer a transparent view of patient attrition and data availability for the respective analyses.

At baseline (Fig. 3A) period, RP-ILD patients (both MDA5 + DM and ASS) exhibited more extensive interstitial lesions and emphysema than non-RP-ILD patients. ASS-RP-ILD showed predominant GGO and reticular pattern, while MDA5 + DM-RP-ILD displayed reticular pattern and emphysema. In rapid progressive period (Fig. 3B), all RP-ILD patients demonstrated marked progression of interstitial lesions and emphysema. ASS-RP-ILD showed increased reticular pattern, whereas MDA5 + DM-RP-ILD exhibited progression of honeycombing, GGO, emphysema, reticular pattern, and consolidation. Slow progressive period (Fig. 3C): Compared to the rapid period, lesion progression slowed. ASS-RP-ILD showed reduced interstitial lesions and increased normal lung volume, while MDA5 + DM-RP-ILD exhibited increased fibrosis (honeycombing, reticular pattern) and reduced GGO/emphysema. Non-Progressive Period (Fig. 3D): Non-RP-ILD patients demonstrated significant increases in normal lung volume and reductions in GGO, consolidation.

Disease subtype comparisons

Rapid Progressive Period (Fig. 4A): MDA5 + DM patients had greater interstitial lesion progression than ASS patients, particularly in fibrotic, inflammatory, and emphysematous features. Slow Progressive Period (Fig. 4B): MDA5 + DM patients showed mild increases in normal lung volume, reticular pattern, and honeycombing with reduced inflammatory lesions/emphysema. ASS patients exhibited reductions in fibrotic and inflammatory lesions. Non-Progressive Period (Fig. 4C): Both subtypes showed increased normal lung volume, with mild fibrosis progression (honeycombing in MDA5 + DM; reticular pattern/honeycombing in ASS) and reduced inflammatory lesions. Figure S2 shows cases of patients with RP-ILD.

Linear mixed-effects model analysis

As shown in Table 4, in RP-ILD patients, particularly ASS, honeycombing, reticular pattern and consolidation increased significantly during the slow progressive period. Non-RP-ILD patients, especially MDA5 + DM, showed significant reductions in GGO. No significant

Table 3 Cumulative deaths and sample sizes for HRCT at follow-up time point by disease subtype*

Patient Subgroups	Total Deceased (*n*)	Deceased at rapid progressive period (*n*)	Deceased at slow progressive period (*n*)	Deceased at non-progressive period (*n*)	HRCT at Rapid Progressive Period Baseline and Follow-up (*n*)	HRCT at Slow Progressive Period Baseline and Follow-up (*n*)	HRCT at None Progressive Period Baseline and Follow-up (*n*)
MDA5 + DM-RP-ILD	20	9	11		103	94	
ASS-RP-ILD	20	2	18		146	144	
MDA5 + DM-non-RP-ILD	1			1			54
ASS-non-RP-ILD	16			16			211

MDA5 + DM Anti-melanoma differentiation-associated gene 5 antibody-positive dermatomyositis, *ASS* Anti-synthetase syndrome, *RP-ILD* Rapidly progressive interstitial lung disease, *non-RP-ILD* Non rapidly progressive interstitial lung disease

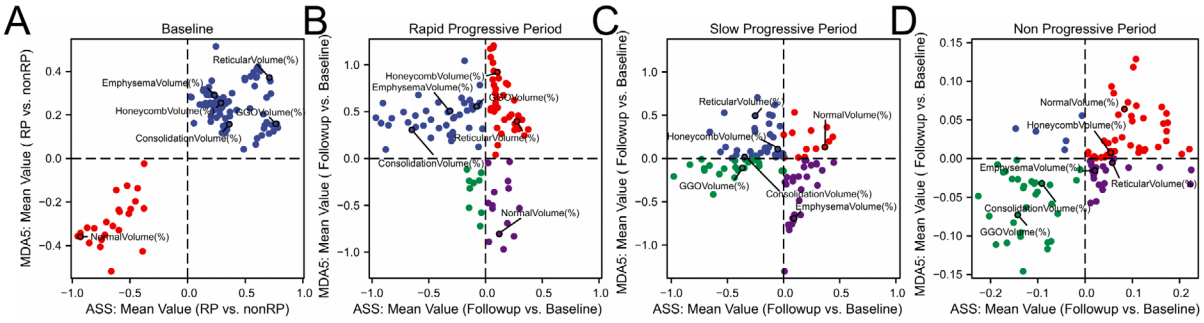

Fig. 3 Comparison of interstitial lesions between MDA5 + DM and ASS across different disease progression stages, including honeycomb, reticular, consolidation, GGO, and emphysema in scatter plot. Each plot represents the average change for one type of interstitial lesion across the whole lung and individual lobes, aggregated at the annotated locations of the corresponding interstitial lesion. The abscissa and ordinate are the difference between the former and the latter in parentheses. The x-axis indicates the difference in imaging changes in ASS, while the y-axis represents the difference in MDA5 + DM. Different colors are used to distinguish four distinct trends of interstitial lesions across the four quadrants. For Figure A: Blue plots indicate cases where both MDA5 + DM and ASS have more extensive imaging lesions. Red plots indicate cases where both MDA5 + DM and ASS have less extensive imaging lesions. For Figures B, C, and D: Red plots indicate cases where the imaging lesions worsened for both MDA5 + DM and ASS. Green plots indicate cases where the imaging lesions improved for both MDA5 + DM and ASS. Blue plots indicate cases where the imaging lesions worsened for MDA5 + DM but improved for ASS. Purple plots indicate cases where the imaging lesions improved for MDA5 + DM but worsened for ASS. **A** Baseline: Compares RP-ILD patients (both MDA5 + DM and ASS) with non-RP-ILD patients, showing more extensive interstitial lesions and emphysema in the RP-ILD groups. ASS-RP-ILD is characterized by GGO and reticulation, while MDA5 + DM-RP-ILD shows greater emphysema and reticulation; (**B**) Rapid Progressive Period in RP-ILD: Shows marked progression of interstitial lesions and emphysema across all RP-ILD patients. ASS-RP-ILD exhibits increased reticulation, while MDA5 + DM-RP-ILD demonstrates progression across multiple patterns including honeycombing, GGO, emphysema, reticulation, and consolidation; (**C**) Slow Progressive Period in RP-ILD: Illustrates slowed lesion progression compared to the rapid phase. ASS-RP-ILD displays reduction in interstitial abnormalities and increased normal lung area, whereas MDA5 + DM-RP-ILD shows increased fibrotic changes (honeycombing and reticulation) with reduction in GGO and emphysema; (**D**) Non Progressive Period in non-RP-ILD: Depicts non-RP-ILD patients, highlighting significant improvement including increased normal lung volume and reduction in GGO and consolidation. *MDA5* Melanoma differentiation-associated protein 5, *ASS* Antisynthetase syndrome, *RP* Rapidly progressive interstitial lung disease, *nonRP* Non rapidly progressive interstitial lung disease, *GGO* Ground glass opacities

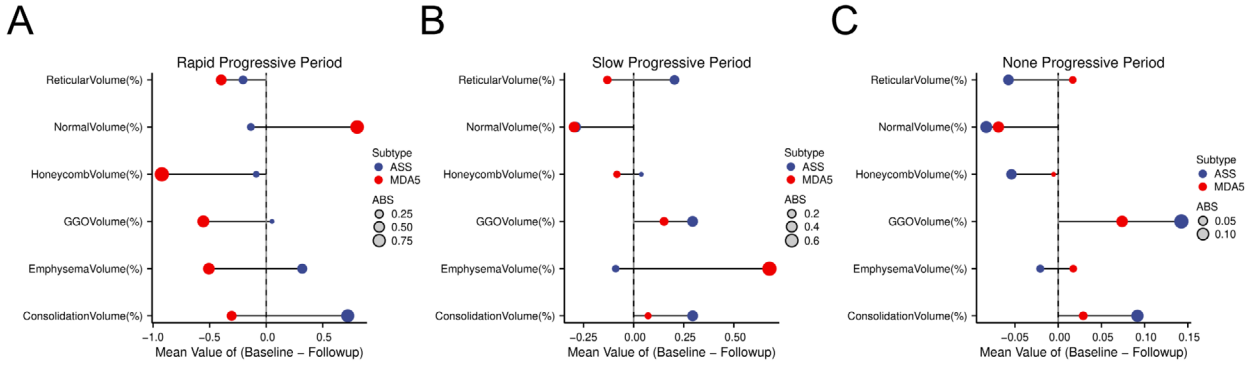

Fig. 4 Comparison of interstitial lesions across different subtypes during various disease progression periods. The horizontal coordinate is the difference between the baseline and the follow-up, where positive values represent improvement in imaging findings and negative values indicate worsening. The blue dots represent ASS, while the red ones represent MDA5 + DM. The size of the dots represents the absolute value of the difference. **A** Rapid Progressive Period in RP-ILD: MDA5 + DM patients exhibited more severe progression of interstitial lesions compared to ASS patients, particularly in fibrotic, inflammatory, and emphysematous features; (**B**) Slow Progressive Period in RP-ILD: MDA5 + DM patients demonstrated mild increases in normal lung volume, reticulation, and honeycombing, alongside reduced inflammatory lesions and emphysema. ASS patients showed improvement with reductions in both fibrotic and inflammatory abnormalities; (**C**) Non Progressive Period in non-RP-ILD: Both subtypes displayed increased normal lung volume and reduction in inflammatory lesions. Mild fibrotic progression was observed: honeycombing in MDA5 + DM, and both reticulation and honeycombing in ASS. *ASS* Antisynthetase syndrome, *MDA5* Melanoma differentiation-associated protein 5, *GGO* Ground glass opacities, *ABS* Absolute value

Table 4 A linear mixed-effect model of interstitial lesions across different subtypes during various disease progression periods*

Group	Period	Honeycomb% Predicted		Reticular% Predicted		Consolidation% Predicted		GGO% Predicted		Emphysema% Predicted	
		Change (95% CI)	*P* Value	Change (95% CI)	*P* Value	Change (95% CI)	*P* Value	Change (95% CI)	*P* Value	Change (95% CI)	*P* Value
All	Rapid Progressive	−0.0055 (−0.0238 to 0.0127)	*0.55*	0.0755 (−0.0158 to 0.1667)	*0.11*	0.0013 (−0.0359 to 0.0384)	*0.95*	0.0818 (−0.1373 to 0.3009)	*0.47*	−0.0404 (−0.1697 to 0.0889)	*0.54*
	Slow Progressive	0.0156 (0.0055 to 0.0258)	***P=0.003***	0.2167 (0.0844 to 0.3490)	***P=0.002***	0.1839 (0.0940 to 0.2737)	***P<0.0001***	−0.1177 (−0.4585 to 0.2230)	*0.50*	−0.0075 (−0.2201 to 0.2050)	*0.94*
	None Progressive	0.0026 (−0.0010 to 0.0063)	*0.16*	0.0036 (−0.0449 to 0.0520)	*0.89*	−0.0055 (−0.0118 to 0.0009)	*0.09*	−0.1168 (−0.2119 to −0.0216)	***P=0.017***	−0.0058 (−0.0211 to 0.0094)	*0.46*
ASS	Rapid Progressive	0.0005 (−0.0074 to 0.0084)	*0.9*	0.0635 (−0.0589 to 0.1859)	*0.31*	−0.0023 (−0.0594 to 0.0548)	*0.94*	0.0596 (−0.2487 to 0.3679)	*0.71*	−0.0499 (−0.1871 to 0.0874)	*0.48*
	Slow Progressive	0.0178 (0.0063 to 0.0293)	***P=0.004***	0.2407 (0.0676 to 0.4139)	***P=0.009***	0.2120 (0.0857 to 0.3383)	***P=0.001***	−0.0726 (−0.4414 to 0.2961)	*0.7*	0.0288 (−0.0324 to 0.0900)	*0.36*
	None Progressive	0.0037 (−0.0013 to 0.0087)	*0.15*	0.0031 (−0.0660 to 0.0723)	*0.93*	−0.0079 (−0.0171 to 0.0013)	*0.10*	−0.1052 (−0.2322 to 0.0218)	*0.11*	−0.0057 (−0.0215 to 0.0100)	*0.48*
MDA5+ DM	Rapid Progressive	−0.0063 (−0.0551 to 0.0425)	*0.8*	0.0622 (−0.0806 to 0.2051)	*0.39*	−0.0060 (−0.0348 to 0.0228)	*0.69*	0.0660 (−0.2283 to 0.3602)	*0.66*	−0.0238 (−0.2952 to 0.2476)	*0.86*
	Slow Progressive	−0.0042 (−0.0274 to 0.0190)	*0.72*	0.0346 (−0.1428 to 0.2119)	*0.71*	−0.0092 (−0.0258 to 0.0074)	*0.28*	−0.4897 (−1.3346 to 0.3553)	*0.26*	−0.2131 (−1.0456 to 0.6194)	*0.62*
	None Progressive	−0.0001 (−0.0042 to 0.0040)	*0.96*	0.0004 (−0.0452 to 0.0459)	*0.99*	−0.0024 (−0.0079 to 0.0031)	*0.39*	−0.1368 (−0.2695 to −0.0040)	***P=0.048***	−0.0048 (−0.0375 to 0.0279)	*0.78*

*Bold values indicate statistical significance at $P < 0.05$. *GGO* Ground glass opacity, *CI* Confidence interval, *ASS* Anti-synthetase syndrome, *MDA5+ DM* Anti-melanoma differentiation-associated gene 5 antibody-positive dermatomyositis

changes were observed during the rapid progressive period. As shown in Table 5, consolidation increased more prominently in the slow progressive period of RP-ILD (especially ASS) compared to the rapid progressive period or non-RP-ILD. Furthermore, during the slow progressive period, RP-ILD exhibited a more pronounced increase in consolidation compared to non-RP-ILD. Further, Figs. 3 and 4 visualize the results summarized in Tables 4 and 5.

Correlation between longitudinal changes in QCT features and pulmonary function

As shown in Fig. 5, reticular pattern and consolidation exhibited strong correlations with VC%, FVC%, and FEV_1%, and moderate correlations with TLC% and DL_{CO}%. Similar trends were observed in both the rapid progressive period of RP-ILD and non-RP-ILD patients. During the slow progressive period of RP-ILD, honeycombing, reticular pattern, and consolidation showed strong correlations with VC%, FVC%, FEV_1%, TLC%, and DL_{CO}%, with fibrotic lesions demonstrating the strongest associations with pulmonary volume and gas exchange function.

Survival analysis

The longitudinal assessment was completed in June 2024, with a final cohort of 514 enrolled patients. Among these, 392 patients (76.3%) completed the study protocol with definitive outcome ascertainment. The median follow-up duration calculated by reverse Kaplan-Meier method was 9.67 years (95% CI: 8.26–12.42), representing time from disease onset to final outcome rather than from study enrollment, as numerous patients experienced disease onset prior to registry accrual. The adverse prognosis included mortality, ICU admission, or lung transplantation. Notably, the prognostic evaluation of imaging findings burden included scans from all disease phases. After adjusting for initial treatment strategies (anti-inflammatory and anti-fibrotic) (Table S4), cox regression with time-dependent interactions (Table 6) revealed that each 1% increase in GGO was associated with a 0.56% higher risk of adverse prognosis (HR: 1.0056, 95% CI: 1.001–1.010). Anti-MDA5 positivity conferred a 2.47-fold higher risk of adverse prognosis compared to ASS (HR: 2.47, 95% CI: 1.15–5.31). The model demonstrated good discrimination (Harrell's C-index: 0.718). Time-dependent HR for GGO showed increasing prognostic impact

Table 5 Difference of interstitial lesions changes in different progression periods*

Group	Period	Honeycomb% Predicted		Reticular% Predicted		Consolidation% Predicted		GGO% Predicted		Emphysema% Predicted	
		Change (95% CI)	*P* Value	Change (95% CI)	*P* Value	Change (95% CI)	*P* Value	Change (95% CI)	*P* Value	Change (95% CI)	*P* Value
All	Rapid-Slow	−0.0178	*0.49*	−0.0697	*0.55*	−0.1647	***P<0.0001***	0.3050	*0.20*	−0.0387	*0.98*
	Rapid-None	−0.0079	*0.49*	0.0343	*0.55*	0.0093	*0.67*	0.1980	*0.20*	−0.0414	*0.98*
	Slow-None	0.0099	*0.49*	0.1040	*0.55*	0.1740	***P<0.0001***	−0.1070	*0.59*	−0.0027	*0.98*
ASS	Rapid-Slow	−0.0100	*0.60*	−0.0782	*0.62*	−0.1951	***P<0.0001***	0.2758	*0.43*	−0.0822	*0.70*
	Rapid-None	−0.0052	*0.60*	0.0376	*0.62*	0.0096	*0.77*	0.1921	*0.43*	−0.0473	*0.70*
	Slow-None	0.0048	*0.60*	0.1158	*0.62*	0.2046	***P<0.0001***	−0.0837	*0.74*	0.0349	*0.71*
MDA5+ DM	Rapid-Slow	−0.0009	*0.99*	0.0535	*0.95*	0.0138	*0.74*	0.4890	*0.47*	0.1708	*0.88*
	Rapid-None	−0.0085	*0.99*	0.0052	*0.95*	−0.0046	*0.74*	0.1100	*0.54*	−0.0228	*0.88*
	Slow-None	−0.0076	*0.99*	−0.0484	*0.95*	−0.0184	*0.74*	−0.3780	*0.47*	−0.1936	*0.88*
ASS-MDA5	Rapid Progressive	0.0030	*0.89*	0.0023	*0.98*	0.0031	*0.94*	0.0177	*0.94*	−0.0260	*0.86*
	Slow Progressive	0.0176	*0.25*	0.2510	*0.21*	0.2320	*0.08*	0.5230	*0.30*	0.2310	*0.46*
	None Progressive	0.003	*0.43*	0.0125	*0.81*	−0.0054	*0.42*	0.0315	*0.75*	−0.0002	*0.99*

*Bold values indicate statistical significance at $P < 0.05$. *GGO* Ground glass opacity, *CI* Confidence interval, *ASS* Anti-synthetase syndrome, *MDA5+ DM* Anti-melanoma differentiation-associated gene 5 antibody-positive dermatomyositis

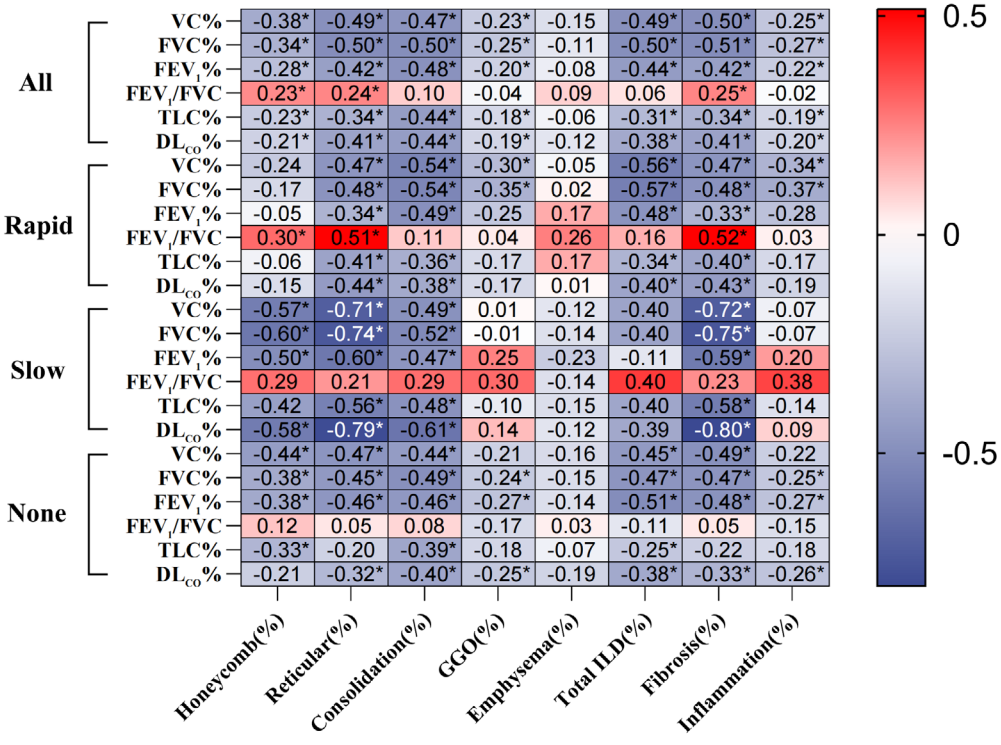

Fig. 5 Correlation of interstitial lesions changes and lung function changes. Total ILD(%) = Honeycomb(%) + Reticular(%) + Consolidation(%) + GGO(%), Fibrosis(%) = Honeycomb(%) + Reticular(%), Inflammation(%) = Consolidation(%) + GGO(%), GGO: ground glass opacity, VC%: the proportion of actual value to the expected value for vital capacity, FVC%: the proportion of actual value to the expected value for forced vital capacity, FEV_1%: the proportion of actual value to the expected value for forced expiratory volume in the first second, FEV_1/FVC: the proportion of forced expiratory volume in the first second to the forced vital capacity, TLC%: the proportion of actual value to the expected value for total lung capacity, DL_{CO}%: the proportion of actual value to the expected value for carbon monoxide diffusing capacity

Table 6 Risk factors for adverse prognosis in idiopathic inflammation myopathy associated interstitial lung disease*

	P-value	HR (95% CI)
Consolidation%	0.357	1.01 (0.99–1.04)
Ground glass opacity%	**0.012**	1.0056 (1.001–1.010)
Reticular%	0.770	1.00 (0.99–1.01)
Honeycomb%	0.270	1.05 (0.96–1.14)
Age	0.251	1.00 (1.00–1.01.00.01)
MDA5	**0.020**	2.47 (1.15–5.31)
Male	0.296	1.43 (0.73–2.80)

* The adverse prognosis included mortality, ICU admission, or lung transplantation. Bold values indicate statistical significance at $P < 0.05$.

HR Hazard ratio, *CI* Confidence interval, *MDA5* Anti-melanoma differentiation associated protein 5

over follow-up, suggesting its role in disease progression. Subgroup analyses for ASS and MDA5 + DM are presented in Tables S5 and S6.

Discussion

This study systematically delineates risk predictors of RP-IIM-ILD, uncovers subtype-specific imaging progression patterns, and proposes dynamic imaging biomarkers through multimodal integration of longitudinal imaging, pulmonary function, and serological data. These findings establish an evidence-based framework for precision stratification in IIM-ILD management.

Risk stratification of RP-ILD

In our cohort, RP-ILD developed in 249 (48.4%) of the 514 patients. Multivariable analysis identified anti-MDA5 antibody seropositivity as the paramount independent predictor of RP-ILD (OR 10.46, 95% CI 3.40–32.22), corroborating its established role in driving aberrant immune activation and accelerated pulmonary parenchymal destruction [29, 30]. Notably, our cohort demonstrated anti-MDA5 positivity conferred a 2.47-fold higher risk of adverse prognosis compared to ASS (HR: 2.47, 95% CI: 1.15–5.31), which concords with Nakashima et al.'s observation of 46% six-month respiratory mortality in MDA5 + DM [31], underscoring the therapeutic recalcitrance characterizing this subgroup [32, 33]. GGO (OR: 1.07, 95% CI: 1.01–1.13) and consolidation on HRCT serve as dual indicators of RP-ILD, with their prognostic significance corroborating previous studies [10, 34–37]. Bilateral diffuse GGO represents the most common early manifestation of MDA5 + DM associated RP-ILD, likely indicative of alveolar septal inflammation or edema [38, 39]. Disease progression may subsequently manifest as consolidation and reticular pattern, indicating fibrotic remodeling or organizing pneumonia [40]. QCT analysis by Xu et al. identified a significant correlation between GGO/consolidation and 6-month mortality in MDA5 + DM patients [18]. PFT in IIM-ILD patients typically demonstrates restrictive ventilatory dysfunction and impaired diffusion capacity [29, 41, 42]. Notably, our study revealed that reduced baseline VC% (OR: 0.91, 95% CI: 0.84–0.98) was associated with the coexistence of extensive GGO and reticular pattern (OR: 1.23, 95% CI: 1.07–1.41), suggesting that the synergistic interaction between mechanical pulmonary restriction and combined inflammatory-fibrotic burden may constitute the core pathophysiological mechanism driving RP-ILD progression.

Dynamic imaging evolution across disease stages

Longitudinal analysis using linear mixed-effects models revealed distinct radiographic trajectories: patients with RP-ILD exhibited significant progression of honeycombing, reticular pattern, and consolidation during the slow progressive period, whereas non-RP-ILD counterparts demonstrated marked regression of GGO. These findings underscore that prior RP-ILD episodes correlate with sustained inflammatory activity, fibrotic transformation, and chronic fibrotic evolution, whereas non-RP-ILD phenotypes are characterized by inflammatory resolution. Our study represents the first application of QCT for dynamic monitoring of interstitial lesion progression in IIM-ILD. Notably, patients with RP-ILD exhibited pathological parallels to idiopathic pulmonary fibrosis, a prototypical progressive fibrotic ILD—sharing persistent chronic inflammation and unchecked fibrogenesis [43, 44]. This comparative analysis challenges the conventional dichotomy between autoimmune-driven and idiopathic ILD, advocating for a unified framework to address shared fibro-inflammatory pathways [45, 46].

Subtype-specific dynamic imaging evolution

Longitudinal imaging analysis revealed distinct progression patterns between ASS and MDA5 + DM. The ASS cohort exhibited a slow progressive period characterized by partial inflammatory resolution but persistent accumulation of consolidations, reflecting chronic inflammation-driven alveolar epithelial injury. It is also important to consider that persistent GGO may not only indicate active inflammation, but also could represent residual post-inflammatory damage, early fine fibrosis, or a mixed state of ongoing alveolar injury and attempted repair [34]. MDA5 + DM cohort demonstrated sustained progression toward HC and reticular pattern-predominant fibrosis during the slow progressive period, suggesting anti-MDA5 antibody-mediated fibroblast transdifferentiation that perpetuates irreversible pulmonary remodeling. It should be noted, however, that this observed radiologic evolution toward a fibrotic-predominant pattern may not solely indicate actively progressive fibrosis, but could also represent a stabilized, post-inflammatory sequela following the acute alveolar injury, particularly in survivors of the initial RP-ILD phase. The

inference of active fibrotic process in MDA5 + DM is based on cross-sectional imaging patterns and requires validation in future prospective studies incorporating longitudinal physiologic data and histopathological correlation to confirm the true activity and progression of fibrosis. Non-RP-ILD subgroup exhibited subclinical fibrotic progression despite inflammatory attenuation, implying persistent microenvironmental dysregulation. Consistent with prior evidence [47–50], ASS typically manifests radiologically as nonspecific interstitial pneumonia (NSIP) or organizing pneumonia (OP) patterns, whereas MDA5 + DM frequently presents with rapidly progressive fibrotic phenotypes or acute lung injury patterns—notably diffuse alveolar damage (DAD). These dichotomous trajectories fundamentally reflect divergent pathomechanisms : ASS progression is driven by "sustained inflammasome activation" versus MDA5 + DM's "post-acute fibrotic reprogramming" [51–53], necessitating subtype-specific therapeutic paradigms.

Functional-radiologic synergy and clinical translation

The strong correlation between fibrotic lesions (honeycombing, reticular pattern) and pulmonary functional parameters (VC%, FVC%, DL_{CO}%) is particularly pronounced during the slow progressive period, underscoring fibrosis as the pivotal driver of irreversible pulmonary impairment. This is corroborated by Roncella et al. [54], who identified inverse correlations between QCT-based ILD scores and both TLC% and DL_{CO}% in ASS. In contrast, GGO and consolidation demonstrate significant functional associations during rapid progressive period, consistent with prior investigations. Ungprasert et al. revealed substantial inverse associations between GGO extent quantified by CALIPER software and both DL_{CO} and TLC [55], while Bae et al. documented negative correlations between longitudinal GGO progression and declining DL_{CO}/FVC values in ASS [56]. These observations suggest that HRCT-detected GGO may reflect concurrent restrictive ventilatory dysfunction and impaired gas exchange. Notably, RP-ILD patients exhibiting diffuse GGO with heterogeneous FDG uptake on PET/CT demonstrate elevated metabolic activity proportional to inflammatory severity [39], supporting GGO as potential biomarkers of active inflammation. Collectively, these findings validate the utility of QCT parameters as non-invasive surrogates for serial pulmonary function testing, particularly enabling dynamic monitoring in critically ill populations where repeated invasive assessments are clinically challenging.

Time-dependent prognostic significance of ground glass opacity burden

This study revealed that the increase in GGO burden (HR: 1.0056, 95% CI: 1.001–1.010) was associated with the elevated mortality risk, with the honeycombing demonstrating a significant upward trend over extended follow-up durations. Prior studies have documented that anti-MDA5 antibody-positive patients may exhibit rapid progression from localized GGO to diffuse pulmonary lesions on chest CT within weeks, often accompanied by precipitous declines in pulmonary function, hypoxemia, and high mortality rates [57, 58]. Notably, GGO exacerbations have been reported to occur more frequently in the usual interstitial pneumonia (UIP) subtype [15]. It is important to acknowledge that our prognostic evaluation of GGO burden incorporated imaging data from all disease phases, including both the acute rapid progressive and post-acute periods. While GGO likely reflects distinct underlying pathologies in these different stages-primarily active inflammation during acute phase versus chronic alveolar damage or evolving fibrosis during slow progression-its cumulative burden throughout the disease course remained a significant predictor of mortality. This study is the first to identify the time-dependent prognostic effect of GGO, suggesting that it may not merely represent acute inflammatory markers but rather reflect persistent alveolar injury or dysregulated repair mechanisms. These findings support the clinical value of serial GGO monitoring across all phases, as it provides integrated prognostic information that may guide long-term management strategies. These findings emphasize that clinicians should remain vigilant regarding long-term pulmonary functional deterioration in patients with progressive GGO, even after surviving the rapid progressive period. Furthermore, this work provides a rationale for serial HRCT monitoring during follow-up to guide timely therapeutic adjustments.

Study limitations

While this study provides the first characterization of heterogeneous imaging trajectories across IIM-ILD subtypes, several limitations warrant cautious interpretation. The single-center design introduces potential selection bias. Another consideration is the presence of missing data for several covariates. Although the proportion of missing values exceeded 30% for some parameters, t-test and logistic regression analysis supported the assumption that the data were Missing Completely at Random (MCAR). Under the MCAR mechanism, the complete-case analysis employed in our study is unlikely to introduce systematic bias into the model estimates, as the missingness is not related to either the observed or unobserved data. Nevertheless, the reduction in sample size due to missingness may have reduced the statistical power of the analyses, potentially affecting the precision and stability of the estimated associations in Table 2. Although we adjusted for initial treatment regimens using statistical models, the diversity and complexity of

subsequent treatments may have introduced residual confounding effects on long-term prognosis and imaging changes, which could not be fully controlled. Further prospective studies are needed for validation. In addition, the short-term fluctuations in emphysema extent observed in our study should be interpreted with caution. These apparent changes are unlikely to represent genuine morphological progression or regression of emphysema, which is typically a permanent structural alteration. Instead, they may reflect the combined effects of algorithmic reclassification in regions with mixed pathological patterns and the potential confounding influence of spontaneous pneumomediastinum-a known complication of IIM-ILD-which can alter parenchymal attenuation and mimic paraseptal emphysema on automated segmentation. Although smoking history was present in a portion of our cohort, the quantitative changes observed in emphysema over time were analyzed across the entire group, and future studies with larger sample sizes could stratify patients based on smoking status. Another limitation of this study is the attrition observed during the follow-up period, primarily attributable to patient mortality. This attrition may introduce attrition bias, potentially leading to an overestimation of the imaging improvement rate or survival rates, as the participants who completed the study may systematically differ from those who were lost to follow-up. Furthermore, the decline in sample size over time may reduce the statistical power of the longitudinal data analyses. Therefore, the interpretation of the results should be approached with caution, considering the potential impact of mortality-related attrition during follow-up. Furthermore, mechanistic insights remain limited—the molecular distinctions between ASS and MDA5 + DM demand clarification through multi-omics investigations. Future multi-center prospective studies should integrate histopathological validation and biomarker profiling to verify the predictive utility of QCT parameters. Additionally, developing precision treatment algorithms tailored to subtype-specific and disease-stage profiles represents a critical next step.

Conclusions

IIM-ILD with prior rapid progression develop chronic fibrotic trajectories with persistent inflammation compared to non-progressive cases. Imaging manifestations of ASS are characterized by sustained inflammatory activity, whereas MDA5 + DM demonstrates post-acute fibrotic remodeling following initial injury. Longitudinal GGO emerges as a critical prognostic indicator, demonstrating time-dependent cumulative risk effects.

Abbreviations

ABS	Absolute value
AI	Artificial intelligence
ALT	Alanine aminotransferase
ARS	Aminoacyl-tRNA synthetase
ASS	Anti-synthetase syndrome
AST	Aspartate aminotransferase
CI	Confidence interval
CK	Creatine kinase
CRP	C-reactive protein
CT	Computed tomography
DAD	Diffuse alveolar damage
DM	Dermatomyositis
DL_{CO}%	Diffusing capacity of the lungs for carbon monoxide (percentage of predicted)
ERS	European Respiratory Society
ESR	Erythrocyte sedimentation rate
FET	Ferritin
FEV_1%	Forced expiratory volume in 1 s (percentage of predicted)
FVC%	Forced vital capacity (percentage of predicted)
GGO	Ground-glass opacity
HC	Honeycombing
HR	Hazard ratio
HRCT	High-resolution computed tomography
ICU	Intensive care unit
IIM-ILD	Idiopathic inflammatory myopathy-associated interstitial lung disease
ILD	Interstitial lung disease
LDH	Lactic dehydrogenase
MDA5 + DM	Anti-melanoma differentiation-associated gene 5 antibody-positive dermatomyositis
MDD	Multidisciplinary discussion
MICE	Multiple Imputation using Chained Equations
OP	Organizing pneumonia
OR	Odds ratio
$PaCO_2$	Arterial carbon dioxide pressure
PaO_2	Arterial oxygen pressure
PFT	Pulmonary function test
QCT	Quantitative computed tomography
RP-ILD	Rapidly progressive interstitial lung disease
SD	Standard deviation
TLC%	Total lung capacity (percentage of predicted)
UIP	Usual Interstitial Pneumonia
VC%	Vital capacity (percentage of predicted)
VIF	Variance Inflation Factor

Supplementary Information

The online version contains supplementary material available at https://doi.org/10.1186/s12890-025-03962-w.

Supplementary Material 1.

Supplementary Material 2.

Supplementary Material 3.

Acknowledgements

Not applicable.

Authors' contributions

(I) Conception and design: ML, HD. (II) Administrative support: ML, HD. (III) Provision of study materials or patients: YH, YR, BX, SW, JG, ML, HD. (IV) Collection and assembly of data: YQ, HW, YN, JW, AL, JD, LX, YH, YR, BX, SW, JG. (V) Data analysis and interpretation: YQ, HW, ML, HD. (VI) Manuscript writing: YQ, HW. (VII) Revision: YQ, HW, ML, HD. (VIII) Final approval of manuscript: All authors.

Funding

Study was supported by the National Key Technologies R&D Program Precision Medicine Research (Nos. 2021YFC2500700 and 2016YFC0901101), and the National Natural Science Foundation of China (No. 81870056).

Data availability
The datasets used and/or analyzed during the current study are available from the corresponding author on reasonable request.

Declarations

Ethics approval and consent to participate
This study was approved by the Ethics Committee of China-Japan Friendship Hospital, and all procedures were conducted in accordance with the Declaration of Helsinki. Written informed consent was obtained from all participants (Approval number: 2017-25).

Consent for publication
Written informed consent for publication of their clinical details and/or images was obtained from the patient.

Competing interests
The authors declare no competing interests.

Author details
[1]Immune Dysfunction and Pulmonary Fibrosis Joint Laboratory for Clinical Medicine, Capital Medical University, Beijing, P.R. China
[2]National Center for Respiratory Medicine; State Key Laboratory of Respiratory Health and Multimorbidity; National Clinical Research Center for Respiratory Diseases; Institute of Respiratory Medicine, Chinese Academy of Medical Sciences; Department of Pulmonary and Critical Care Medicine, Center of Respiratory Medicine, China-Japan Friendship Hospital, No. 2 Yinghua Dong Street, Chao Yang District, Beijing 100029, P.R. China
[3]China-Japan Friendship Hospital (Institute of Clinical Medical Sciences), Chinese Academy of Medical Sciences & Peking Union Medical College, Beijing, China
[4]Department of Radiology, China-Japan Friendship Hospital, No. 2 Yinghua Dong Street, Chao Yang District, Beijing 100029, China

Received: 16 July 2025 / Accepted: 25 September 2025
Published online: 03 November 2025

References

1. Douglas WW. Polymyositis-dermatomyositis-associated interstitial lung. Am J Respir Crit Care Med. 2001.
2. Schmidt J. Current classification and management of inflammatory myopathies. J Neuromuscul Dis. 2018;5(2):109–29.
3. Betteridge Z, McHugh N. Myositis-specific autoantibodies: an important tool to support diagnosis of myositis. J Intern Med. 2016;280(1):8–23.
4. Lia Y, Fana Y, Wanga Y, Yanga S, Dua X, Yea Q. Phenotypic clusters and survival analyses in interstitial pneumonia with myositis-specific autoantibodies. Sarcoidosis Vasc Diffuse Lung Dis. 2022;38(4):e2021047.
5. Pinal-Fernandez I, Casal-Dominguez M, Mammen AL. Immune-mediated necrotizing myopathy. Curr Rheumatol Rep. 2018;20(4):21.
6. Shi J, Li S, Yang H, Zhang Y, Peng Q, Lu X, et al. Clinical profiles and prognosis of patients with distinct antisynthetase autoantibodies. J Rheumatol. 2017;44(7):1051–7.
7. Hamaguchi Y, Fujimoto M, Matsushita T, Kaji K, Komura K, Hasegawa M, et al. Common and distinct clinical features in adult patients with anti-aminoacyl-tRNA synthetase antibodies: heterogeneity within the syndrome. PLoS ONE. 2013;8(4):e60442.
8. Zuo Y, Ye L, Chen F, Shen Y, Lu X, Wang G, et al. Different multivariable risk factors for rapid progressive interstitial lung disease in Anti-MDA5 positive dermatomyositis and Anti-Synthetase syndrome. Front Immunol. 2022;13:845988.
9. Raghu G, Remy-Jardin M, Richeldi L, Thomson CC, Inoue Y, Johkoh T, et al. Idiopathic pulmonary fibrosis (an Update) and progressive pulmonary fibrosis in adults: an official ATS/ERS/JRS/ALAT clinical practice guideline. Am J Respir Crit Care Med. 2022;205(9):e18–47.
10. Won Huh J, Soon Kim D, Keun Lee C, Yoo B, Bum Seo J, Kitaichi M, et al. Two distinct clinical types of interstitial lung disease associated with polymyositis-dermatomyositis. Respir Med. 2007;101(8):1761–9.
11. Jacob J, Bartholmai BJ, Rajagopalan S, Kokosi M, Nair A, Karwoski R, et al. Mortality prediction in idiopathic pulmonary fibrosis: evaluation of computer-based CT analysis with conventional severity measures. Eur Respir J. 2017. https://doi.org/10.1183/13993003.01011-2016
12. Clukers J, Lanclus M, Mignot B, Van Holsbeke C, Roseman J, Porter S, et al. Quantitative CT analysis using functional imaging is superior in describing disease progression in idiopathic pulmonary fibrosis compared to forced vital capacity. Respir Res. 2018;19(1):213.
13. Yeo J, Yoon SH, Kim JY, Lee JS, Lee EY, Goo JM, et al. Quantitative interstitial lung disease scores in idiopathic inflammatory myopathies: longitudinal changes and clinical implications. Rheumatology (Oxford). 2023. https://doi.org/10.1093/rheumatology/kead122.
14. Handa T, Tanizawa K, Oguma T, Uozumi R, Watanabe K, Tanabe N, et al. Novel artificial Intelligence-based technology for chest computed tomography analysis of idiopathic pulmonary fibrosis. Ann Am Thorac Soc. 2022;19(3):399–406.
15. Yeo J, Yoon SH, Kim JY, Lee JS, Lee EY, Goo JM, et al. Quantitative interstitial lung disease scores in idiopathic inflammatory myopathies: longitudinal changes and clinical implications. Rheumatology (Oxford). 2023;62(11):3690–9.
16. Laporte A, Mariampillai K, Allenbach Y, Pasi N, Donciu V, Toledano D, et al. Idiopathic inflammatory myopathies: CT characteristics of interstitial lung disease and their association(s) with myositis-specific autoantibodies. Eur Radiol. 2022;32(5):3480–9.
17. Xu W, Wu W, Zheng Y, Chen Z, Tao X, Zhang D, et al. A computed tomography Radiomics-based prediction model on interstitial lung disease in Anti-MDA5-Positive dermatomyositis. Front Med. 2021;8:768052.
18. Xu W, Wu W, Zhang D, Chen Z, Tao X, Zhao J, et al. A novel CT scoring method predicts the prognosis of interstitial lung disease associated with anti-MDA5 positive dermatomyositis. Sci Rep. 2021;11(1):17070.
19. Mathai SC, Danoff SK. Management of interstitial lung disease associated with connective tissue disease. BMJ. 2016;352:h6819.
20. Travis WD, Costabel U, Hansell DM, King TE Jr., Lynch DA, Nicholson AG, et al. An official American Thoracic Society/European Respiratory Society statement: update of the international multidisciplinary classification of the idiopathic interstitial pneumonias. Am J Respir Crit Care Med. 2013;188(6):733–48.
21. Mammen AL, Allenbach Y, Stenzel W, Benveniste O, Group EtWS. 239th ENMC international workshop: classification of dermatomyositis, Amsterdam, the Netherlands, 14–16 december 2018. Neuromuscul Disord. 2020;30(1):70–92.
22. Bohan A. JBP. Polymyositis and dermatomyositis(first of two parts). the new england journal of medicine 1975.
23. Cavagna L, Trallero-Araguás E, Meloni F, Cavazzana I, Rojas-Serrano J, Feist E, et al. Influence of antisynthetase antibodies specificities on antisynthetase syndrome clinical spectrum time course. J Clin Med. 2019. https://doi.org/10.3390/jcm8112013
24. Raghu G, Collard HR, Egan JJ, Martinez FJ, Behr J, Brown KK, et al. An official ATS/ERS/JRS/ALAT statement: idiopathic pulmonary fibrosis: evidence-based guidelines for diagnosis and management. Am J Respir Crit Care Med. 2011;183(6):788–824.
25. Stanojevic S, Kaminsky DA, Miller MR, Thompson B, Aliverti A, Barjaktarevic I, et al. ERS/ATS technical standard on interpretive strategies for routine lung function tests. Eur Respir J. 2022. https://doi.org/10.1183/13993003.01499-2021
26. Miller MR, Hankinson J, Brusasco V, Burgos F, Casaburi R, Coates A, et al. Standardisation of spirometry. Eur Respir J. 2005;26(2):319–38.
27. Zhang XL, Zhang L, Li YM, Xiang BY, Han T, Wang Y, et al. Multidimensional assessment and cluster analysis for OSA phenotyping. J Clin Sleep Med. 2022;18(7):1779–88.
28. Sterne JA, White IR, Carlin JB, Spratt M, Royston P, Kenward MG, et al. Multiple imputation for missing data in epidemiological and clinical research: potential and pitfalls. BMJ. 2009;338:b2393.
29. Fathi M, Vikgren J, Boijsen M, Tylen U, Jorfeldt L, Tornling G, et al. Interstitial lung disease in polymyositis and dermatomyositis: longitudinal evaluation by pulmonary function and radiology. Arthritis Rheum. 2008;59(5):677–85.
30. Li S, Sun Y, Shao C, Huang H, Wang Q, Xu K, et al. Prognosis of adult idiopathic inflammatory myopathy-associated interstitial lung disease: a retrospective study of 679 adult cases. Rheumatology (Oxford). 2021;60(3):1195–204.
31. Nakashima R, Imura Y, Kobayashi S, Yukawa N, Yoshifuji H, Nojima T, et al. The RIG-I-like receptor IFIH1/MDA5 is a dermatomyositis-specific autoantigen identified by the anti-CADM-140 antibody. Rheumatology (Oxford). 2010;49(3):433–40.

32. Chen Z, Cao M, Plana MN, Liang J, Cai H, Kuwana M, et al. Utility of anti-melanoma differentiation-associated gene 5 antibody measurement in identifying patients with dermatomyositis and a high risk for developing rapidly progressive interstitial lung disease: a review of the literature and a meta-analysis. Arthritis Care Res (Hoboken). 2013;65(8):1316–24.
33. Vuillard C, Pineton de Chambrun M, de Prost N, Guerin C, Schmidt M, Dargent A, et al. Clinical features and outcome of patients with acute respiratory failure revealing anti-synthetase or anti-MDA-5 dermato-pulmonary syndrome: a French multicenter retrospective study. Ann Intensive Care. 2018;8(1):87.
34. Chen X, Jiang W, Jin Q, Peng Q, Zhang L, Lin S, et al. Clinical, radiological and pathological features of anti-MDA5 antibody-associated interstitial lung disease. RMD Open. 2023. https://doi.org/10.1136/rmdopen-2023-003150
35. Koreeda Y, Higashimoto I, Yamamoto M, Takahashi M, Kaji K, Fujimoto M, et al. Clinical and pathological findings of interstitial lung disease patients with anti-aminoacyl-tRNA synthetase autoantibodies. Intern Med. 2010;49(5):361–9.
36. Hayashi S. High resolution computed tomography characterization of interstitial lung diseases in polymyositis/dermatomyositis. J Rheumatol. 2008.
37. Tanizawa K, Handa T, Nakashima R, Kubo T, Hosono Y, Aihara K, et al. The prognostic value of HRCT in myositis-associated interstitial lung disease. Respir Med. 2013;107(5):745–52.
38. Abu-Rumeileh S, Marrani E, Maniscalco V, Maccora I, Pagnini I, Mastrolia MV, et al. Lung involvement in juvenile idiopathic inflammatory myopathy: a systematic review. Autoimmun Rev. 2023;22(10):103416.
39. Zhang J, Dong A. FDG PET/CT findings of rapidly progressive interstitial lung disease in a patient with anti-MDA5 dermatomyositis. Clin Nucl Med. 2025;50(1):80–2.
40. Ichimura Y, Konishi R, Shobo M, Tanaka R, Kubota N, Kayama H, et al. Autoimmunity against melanoma differentiation-associated gene 5 induces interstitial lung disease mimicking dermatomyositis in mice. Proc Natl Acad Sci U S A. 2024;121(16):e2313070121.
41. Marie I, Josse S, Hatron PY, Dominique S, Hachulla E, Janvresse A, et al. Interstitial lung disease in anti-Jo-1 patients with antisynthetase syndrome. Arthritis Care Res (Hoboken). 2013;65(5):800–8.
42. Tillie-Leblond I, Wislez M, Valeyre D, Crestani B, Rabbat A, Israel-Biet D, et al. Interstitial lung disease and anti-Jo-1 antibodies: difference between acute and gradual onset. Thorax. 2008;63(1):53–9.
43. Forde L, Gogoi D, Baird R, McCarthy C, Keane MP, Reeves EP, et al. Does adenosine triphosphate via purinergic receptor signalling fuel pulmonary fibrosis? J Innate Immun. 2025;17(1):44–55.
44. Shadid A, Rich HE, DeVaughn H, Domozhirov A, Doursout MF, Weng-Mills T, et al. Persistent microbial infections and idiopathic pulmonary fibrosis - an insight into non-typeable haemophilus influenza pathogenesis. Front Cell Infect Microbiol. 2024;14:1479801.
45. Crowley LE, Stockley RA, Thickett DR, Dosanjh D, Scott A, Parekh D. Neutrophil dynamics in pulmonary fibrosis: pathophysiological and therapeutic perspectives. Eur Respir Rev. 2024;33:174.
46. Nguyen HN, Jeong Y, Kim Y, Kamiya M, Kim Y, Athar H, et al. Leukemia inhibitory factor (LIF) receptor amplifies pathogenic activation of fibroblasts in lung fibrosis. Proc Natl Acad Sci U S A. 2024;121(50):e2401899121.
47. Moussa N, Gargouri R, Snoussi M, Khemakhem R, Bahloul Z, Kammoun S. Nonspecific interstitial pneumonia revealing an antisynthetase syndrome. Monaldi Arch Chest Dis. 2022;93(3).
48. Stenzel W, Mammen AL, Gallay L, Holzer MT, Kleefeld F, Benveniste O, et al. 273rd ENMC international workshop: clinico-sero-morphological classification of the Antisynthetase syndrome. Amsterdam, The Netherlands, 27–29 October 2023. Neuromuscul Disord. 2024;45:104453.
49. Wu W, Collins BF, Gardner GC, Hippe DS, Ho LA, Raghu G, et al. Antisynthetase syndrome-related interstitial lung disease (ASyS-ILD): longitudinal imaging findings. Eur Radiol. 2023;33(7):4746–57.
50. Sehgal S, Patel A, Chatterjee S, Fernandez AP, Farver C, Yadav R et al. Idiopathic inflammatory myopathies related lung disease in adults. Lancet Respir Med. 2024.
51. Wischnewski S, Rausch HW, Ikenaga C, Leipe J, Lloyd TE, Schirmer L. Emerging mechanisms and therapeutics in inflammatory muscle diseases. Trends Pharmacol Sci. 2025. https://doi.org/10.1016/j.tips.2025.01.005.
52. Liu Y, Feng S, Liu X, Tang Y, Li X, Luo C, et al. IFN-beta and EIF2AK2 are potential biomarkers for interstitial lung disease in anti-MDA5 positive dermatomyositis. Rheumatology (Oxford). 2023;62(11):3724–31.
53. He J, Liu Z, Cao Y, Zhang X, Yi C, Zhou Y, et al. Single-cell landscape of peripheral immune response in patients with anti-melanoma differentiation-associated gene 5 dermatomyositis. Rheumatology (Oxford). 2024;63(8):2284–94.
54. Roncella C, Barsotti S, Valentini A, Cavagna L, Castellana R, Cioffi E, et al. Evaluation of interstitial lung disease in idiopathic inflammatory myopathies through semiquantitative and quantitative analysis of lung computed tomography. J Thorac Imaging. 2022;37(5):344–51.
55. Ungprasert P, Wilton KM, Ernste FC, Kalra S, Crowson CS, Rajagopalan S, et al. Novel assessment of interstitial lung disease using the Computer-Aided lung informatics for pathology evaluation and rating (CALIPER) software system in idiopathic inflammatory myopathies. Lung. 2017;195(5):545–52.
56. Bae SS, Abtin F, Kim G, Markovic D, Chan C, Moghadam-Kia S, et al. Relationship between high-resolution computed tomography quantitative imaging analysis and physiological and clinical features in antisynthetase syndrome-related interstitial lung disease. RMD Open. 2024. https://doi.org/10.1136/rmdopen-2024-004592
57. Biddle K, Agaoglu E, Brent G, Adam J, Nockels R, Loveridge A, et al. Two challenging cases of anti-MDA-5 dermatomyositis with rapidly progressive interstitial lung disease. Oxf Med Case Rep. 2024;2024(6):omae061.
58. Xiao F, Chen F, Li D, Zheng S, Liang X, Wu J, et al. Severe interstitial lung disease risk prediction in anti-melanoma differentiation-associated protein 5 positive dermatomyositis: the STRAD-Ro52 model. Ann Med. 2025;57(1):2440621.

Publisher's Note